Two New One-Dimensional Antiferromagnetic Nickel(II) Complexes Bridged by Azido Ligands in Cis Positions. Effect of the Counteranion on the Magnetic Properties

Joan Ribas,*[1a] Montserrat Monfort,[1a] Carmen Diaz,[1a] Carles Bastos,[1a] Christine Mer,[1a,b] and Xavier Solans[1c]

Departament de Química Inorgànica, Universitat de Barcelona, Diagonal 647, 08028-Barcelona, Spain, and Departament de Cristal.lografia i Mineralogia, Universitat de Barcelona, Martí i Franqués, s/n, 08028-Barcelona, Spain

Received June 23, 1994[⊗]

Two new nickel(II) polynuclear end-to-end azide bridged compounds were synthesized and characterized: $[NiL_2(\mu\text{-}N_3)]_n(ClO_4)_n$ (**1**) and $[NiL_2(\mu\text{-}N_3)]_n(PF_6)_n$ (**2**); L = 1,2-diamino-2-methylpropane. The crystal structures of **1** and **2** were solved. Complex **1** crystallizes in the orthorhombic system, space group $P2_12_12_1$, with fw = 376.49, a = 7.392(2) Å, b = 13.879(3) Å, c = 16.178(3) Å, V = 1660(1) Å^3, Z = 4, R = 0.049, and R_w = 0.052. Complex **2** crystallizes in the orthorhombic system, space group $Pbn2_1$, with fw = 422.00, a = 17.022(3) Å, b = 13.760(2) Å, c = 7.550(1) Å, V = 1768.4(8) Å^3, Z = 4, R = 0.057, and R_w = 0.060. In the two complexes, the nickel atom is situated in similar distorted octahedral environments. The Ni−Ni distances are 5.313 Å for **1** and 5.335 Å for **2**. The two complexes are similar and may be described as helicoidal chains. The only marked difference is that the ClO_4^- chain is more compact. The magnetic properties of the two compounds were studied by susceptibility measurements vs temperature. The χ_M vs T plot for **1** shows the typical shape for one antiferromagnetically coupled nickel(II) one-dimensional complex with a maximum near 30 K. In contrast, the absence of a maximum down to 4 K in the χ_M vs T plot for **2** indicates low antiferromagnetic coupling. From the spin Hamiltonian $-J\sum S_iS_j$, J values for **1** and **2**, were −16.8 and −3.2 cm^{-1}, respectively. This difference in magnetic behavior may be explained in terms of the distortion of each Ni(II) ion, the compactness of the chains, and the possibly different magnetic pathways from a molecular orbital point of view.

Introduction

The azido anion is a versatile bridging ligand which can coordinate Ni(II) ions, giving dinuclear complexes in either end-to-end[2−5] or end-on[6−9] form, tetranuclear complexes in end-on[10] form, 1-D complexes in end-to-end form (uniform chains[11−13] and alternating chains[14]) or in end-on[15] form, and, finally, 1-D and bidimensional complexes in which both end-to-end and end-on forms are present.[16] Focusing our attention on one-dimensional antiferromagnetic systems, we find that almost all the complexes reported to date present the azido bridging ligand in a trans position, allowing a very good pathway for the magnetic exchange via d_{z^2} orbitals. For this reason, magneto−structural correlations have recently been reported,[12,13] in which the J parameter (in cm^{-1}) is well correlated to the Ni−N−N angle and the Ni−N_3−Ni torsion angle. Only a few similar complexes with the azido bridging ligand in a cis position have been reported,[13,17] and similar molecular orbital calculations were performed indicating the correlation between J and the above-mentioned parameters. The only important difference is the lower J value found in these theoretical predictions. On the other hand, in the cis position, there are two possibilities for the magnetic pathway: $d_{xy}-d_{xy}$ or $d_{xy}-d_{z^2}$. In the first case, the possibility of strong antiferromagnetic coupling is almost the same as for trans azido systems, but in the second case, the $d_{xy}-d_{z^2}$ pathway strongly reduces the antiferromagnetic coupling. In a given complex, both pathways could be operative, due to the geometrical distortions in the Ni(II) atoms. Consequently, a wide range of J parameters could be expected in these systems. The difficulty is synthesizing these cis complexes instead the trans analogs. Working with 1,2-diamino-2-methylpropane (L), we were able to synthesize two new cis complexes, $[NiL_2(\mu\text{-}N_3)]_n(ClO_4)_n$ (**1**) and $[NiL_2(\mu\text{-}N_3)]_n(PF_6)_n$ (**2**), which were similar in structure but different in magnetic behavior. We now present some hypotheses to explain this anomalous behavior: the counteranion effect, which introduces a different compactness

⊗ Abstract published in *Advance ACS Abstracts,* September 1, 1995.

(1) (a) Department of Inorganic Chemistry, University of Barcelona. (b) Current address: Institut Universitaire de Technologie, Lannion, France. (c) Department of Crystallography, University of Barcelona.
(2) Wagner, F.; Mocella, M. T.; D'Aniello, M. J.; Wang, A. J. H.; Barefield, E. K. *J. Am. Chem. Soc.* **1974**, *96*, 2625.
(3) Pierpont, C. G.; Hendrickson, D. N.; Duggan, D. M.; Wagner, F.; Barefield, E. K. *Inorg. Chem.* **1975**, *14*, 604.
(4) Chaudhuri, P.; Guttman, M.; Ventur, D.; Wieghardt, K.; Nuber, B.; Weiss, J. J. *J. Chem. Soc. Chem. Commun.* **1985**, 1618.
(5) Ribas, J.; Monfort, M.; Diaz, C.; Bastos, C.; Solans, X. *Inorg. Chem.* **1993**, *32*, 3557.
(6) Arriortua, M. I.; Cortés, A. R.; Lezama, L.; Rojo, T.; Solans, X. *Inorg. Chim. Acta* **1990**, *174*, 263.
(7) Escuer, A.; Vicente, R.; Ribas, J. *J. Magn. Magn. Mater.* **1992**, *110*, 181.
(8) Vicente, R.; Escuer, E.; Ribas, J.; Fallah, M. S.; Solans, X.; Font-Bardía, M. *Inorg. Chem.* **1993**, *32*, 1920 and references therein.
(9) Cortés, R.; Ruiz de Larramendi, J. I.; Lezama, L.; Rojo, T.; Urtiaga, K.; Arriortua, M. I. *J. Chem. Soc., Dalton Trans.* **1992**, 2723.
(10) Ribas, J.; Monfort, M.; Costa, R.; Solans, X. *Inorg. Chem.* **1993**, *32*, 695.
(11) Escuer, A.; Vicente, R.; Ribas, J.; El Fallah, M. S.; Solans, X. *Inorg. Chem.* **1993**, *32*, 1033.
(12) Escuer, A.; Vicente, R.; Ribas, J.; El Fallah, M. S.; Solans, X.; Font-Bardia, M. *Inorg. Chem.* **1993**, *32*, 3727.
(13) Escuer, A.; Vicente, R.; Ribas, J.; El Fallah, M. S.; Solans, X.; Font-Bardía, M. *Inorg. Chem.* **1994**, *33*, 1842.
(14) Vicente, R.; Escuer, A.; Ribas, J.; Solans, X. *Inorg. Chem.* **1992**, *31*, 1726.
(15) Ribas, J.; Monfort, M.; Diaz, C.; Bastos, C.; Solans, X. *Inorg. Chem.* **1994**, *33*, 484.
(16) (a) Monfort, M.; Ribas, J.; Solans, X. *J. Chem. Soc. Chem. Commun.* **1993**, 350. (b) Ribas, J.; Monfort, M.; Solans, X.; Drillon, M. *Inorg. Chem.* **1994**, *33*, 742. (c) Ribas, J.; Monfort, M.; Ghosh, B. K.; Solans, X. *Angew. Chem., Int. Ed. Engl.* **1994**, *33*, 2087.
(17) Cortés, R.; Urtiaga, K.; Lezama, L.; Pizarro, J. L.; Goñi, A.; Arriortua, M. L.; Rojo, T. *Inorg. Chem.* **1994**, *33*, 4009.

0020-1669/95/1334-4986$09.00/0

Table 1. Crystallographic Data for $[Ni(1,2\text{-diamino-2-methylpropane})_2(\mu\text{-}N_3)]_n(ClO_4)_n$ (**1**) and $[Ni(1,2\text{-diamino-2-methylpropane})_2(\mu\text{-}N_3)]_n(PF_6)_n$ (**2**)

	1	**2**
chem formula	$C_8H_{24}ClN_7NiO_4$	$C_8H_{24}F_6N_7NiP$
fw	376.49	422.00
T	room temp	room temp
space group	$P2_12_12_1$	$Pbn2_1$
a, Å	7.392(2)	17.022(3)
b, Å	13.879(3)	13.760(2)
c, Å	16.178(3)	7.550(1)
V, Å^3	1660(1)	1768.4(8)
Z	4	4
λ(Mo Kα), Å	0.710 69	0.710 69
d_{cal}, g·cm^{-3}	1.506	1.585
μ(Mo Kα), cm^{-1}	13.53	12.56
R^a	0.049	0.057
$R_w{}^b$	0.052	0.060

^{a} $R = \sum||F_o| - |F_c||/\sum|F_o|$. ^{b} $R_w = [\sum w(|F_o| - |F_c|)^2/\sum w|F_o|^2]^{1/2}$.

in the helicoidal structures, and the electronic factors related to the molecular orbital pathway in each case.

Experimental Section

Caution!. Perchlorate and azide complexes of metal ions are potentially explosive. Only a small amount of material should be prepared, and it should be handled with caution.

Synthesis of the New Complexes. $[Ni(1,2\text{-diamino-2-methylpropane})_2(\mu\text{-}N_3)]_n(ClO_4)_n$ (1). To an aqueous solution of 1 mmol (0.365 g) of $Ni(ClO_4)_2{\cdot}6H_2O$ and 2 mmol (0.176 g) of 1,2-diamino-2-methylpropane in 30 mL of water was added an aqueous solution of 1 mmol (0.065 g) of NaN_3. After filtration to remove any impurity, the aqueous solutions were left undisturbed, and well-formed blue crystals of **1** were obtained after several days. The elemental analyses (C, N, H, Ni) were consistent with the formulation $C_8H_{24}ClN_7O_4Ni$. Anal. Calcd/found: C, 25.52/25.5; H, 6.42/6.4; N, 26.04/26.1; Ni, 15.59/15.6.

$[Ni(1,2\text{-diamino-2-methylpropane})_2(\mu\text{-}N_3)]_n(PF_6)_n$ (2). To an aqueous solution of 1 mmol (0.291 g) of $Ni(NO_3)_2{\cdot}6H_2O$ and 2 mmol (0.176 g) of 1,2-diamino-2-methylpropane in 30 mL of water was added an aqueous solution of 1 mmol (0.065 g) of NaN_3. After filtration to remove any impurity, 1.2 mmol (0.220 g) of KPF_6 was added with continuous stirring. The aqueous solutions were left undisturbed, and well-formed blue crystals of **2** were obtained after several days. The elemental analyses (C, N, H, Ni) were consistent with the formulation $C_8H_{24}F_6N_7NiP$. Anal. Calcd/found: C, 22.76/22.7; H, 5.73/5.8; N, 23.23/23.2; Ni, 13.91/14.0.

Physical Measurements. Magnetic measurements were carried out on polycrystalline samples with a pendulum type-magnetometer (MANICS DSM8) equipped with a helium continuous-flow cryostat, working in the temperature range 300−4 K, and a Bruker BE15 electromagnet. The magnetic field was approximately 15 000 G. The instrument was calibrated by magnetization measurements of a standard ferrite. Diamagnetic corrections were estimated from Pascal constants.

Crystal Data Collection and Refinement. Crystals of **1** (0.15 × 0.10 × 0.20 mm) and **2** (0.1 × 0.1 × 0.2 mm) were selected and mounted on an Enraf-Nonius CAD4 four-circle diffractometer for **1** and on a Philips PW-1100 four-circle diffractometer for **2**. Unit cell parameters were determined from automatic centering of 25 reflections ($12 \le \theta \le 22°$ for **1** and $8 \le \theta \le 12°$ for **2**) and refined by least-squares methods. Intensities were collected with graphite-monochromatized Mo Kα radiation, using the $\omega/2\theta$ scan technique. For **1**, 5387 reflections were measured in the range $2 \le \theta \le 30°$, 2275 of which were assumed to be observed by applying the condition $I \ge 2.5\sigma(I)$. For **2**, 1687 reflections were measured in the range $2 \le \theta \le 25°$, 1388 of which were assumed to be observed by applying the same condition. Three reflections were measured every 2 h as orientation and intensity control; significant intensity decay was not observed. Lorentz−polarization corrections but not absorption corrections were made. The crystallographic data are shown in Table 1. The crystal structures were solved by Patterson syntheses using the SHELXS computer program[18] and refined by full-matrix least-squares methods using the SHELX76[19] computer programs. The function minimized was $\sum w[|F_o| - |F_c|]^2$ where $w = [\sigma^2(F_o) + k|F_o|^2]^{-1}$ and $k = 0.013$ for **1** and 0.018 for **2**. f, f', and f'' were taken from ref 20. For **1**, two oxygen atoms of ClO_4^- were located in disordered positions; an occupancy factor of 0.5 was assigned according to the height of the Fourier synthesis. Thirteen H atoms were located from a difference synthesis, and the remaining were computed. All were refined with an overall isotropic temperature factor, using a riding model. For **2**, the fluorine atoms of PF_6^- and the two C atoms of the two methyl groups were located in disordered positions; an occupancy factor of 0.5 was assigned according to the height of the Fourier synthesis. The positions of 16 H atoms were computed and refined with an overall isotropic factor, using a riding model. For **1**, the final R factor was 0.049 ($R_w = 0.052$) for all observed reflections; 248 parameters were refined; maximum shift/esd = 0.06; maximum and minimum peaks in the final difference synthesis were 0.3 and −0.3 e Å^{-3}, respectively. For **2**, the final R factor was 0.057 ($R_w = 0.060$) for all observed reflections; 280 parameters were refined; maximum shift/esd = 0.1; maximum and minimum peaks in the final difference syntheses were again 0.3 and −0.3 eÅ^{-3}, respectively. Final atomic coordinates for **1** and **2** are given in Tables 2 and 3, respectively.

Table 2. Positional Parameters and Equivalent Isotropic Thermal Parameters with Their Estimated Standard Deviations for $[NiL_2(\mu\text{-}N_3)]_n(ClO_4)_n$ (**1**)

	x/a	y/b	z/c	B_{eq},^{a} Å^2
Ni	89947(7)	13065(4)	94140(3)	2.20(2)
Cl	5752(18)	8737(10)	29869(9)	3.51(5)
N1	8954(7)	2775(3)	9857(3)	3.40(18)
N2	10206(5)	3280(3)	9923(3)	2.52(15)
N3	6426(7)	1184(4)	10020(4)	4.07(21)
N4	11326(6)	1574(3)	8671(3)	2.76(15)
N5	7677(6)	1600(4)	8304(3)	3.39(18)
N6	9045(7)	−214(3)	9233(2)	2.72(14)
N7	10540(7)	923(3)	10453(3)	3.11(17)
C1	10795(9)	1972(4)	7846(3)	3.13(20)
C2	8988(11)	1518(5)	7617(3)	4.11(25)
C3	10595(10)	3059(5)	7902(4)	4.08(26)
C4	12222(15)	1715(7)	7198(5)	5.70(39)
C5	9741(8)	−706(4)	9992(3)	2.99(18)
C6	11244(8)	−64(4)	10333(4)	3.22(21)
C7	10531(13)	−1703(5)	9756(5)	4.75(30)
C8	8224(11)	−861(6)	10607(5)	4.57(30)
O1	795(47)	1489(27)	2476(20)	13.83(191)
O2	213(22)	1422(31)	3634(16)	12.97(171)
O3	2309(9)	442(5)	3161(5)	6.65(32)
O4	−640(11)	159(6)	2655(6)	8.68(46)
O1′	10414(18)	−3699(16)	11327(10)	5.83(65)
O2′	9254(23)	−3388(9)	12695(9)	3.96(42)

^{a} $B_{eq} = (8\pi/3)U_{ij}A_i{}^*A_j{}^*A_i{}^*A_j$.

Results and Discussion

Description of the Structures. Both structures consist of 1-D nickel−azido chains isolated by ClO_4^- and PF_6^- for **1** and **2**, respectively, found in the interchain space. Hydrogen bonds are present between the chains and the counteranion groups. The minimum distances are O3−N4 = 3.087 Å and O4−N5 = 3.054 Å for **1** and N4−F3 = 3.110 Å and N4−F3′ = 3.075 for **2**, respectively. In the chain structures, each Ni(II) atom is coordinated by two bidentate 1,2-diamino-2-methylpropane and two azido ligands in a distorted octahedral cis arrangement.

$[NiL_2(\mu\text{-}N_3)]_n(ClO_4)_n$ (1). A labeled scheme is shown in Figure 1. The main bond lengths and angles are listed in Table 4. Other distances and angles may be found in the Supporting Information. The nickel atom occupies a distorted octahedral

(18) Sheldrick, G. M. *Acta Crystallogr.* **1990**, *A46*, 467.
(19) Sheldrick, G. M. SHELX. A computer program for crystal structure determination. University of Cambridge, England **1976**.
(20) *International Tables for X-ray Crystallography;* Kynoch Press: Birmingham, England, **1976**.

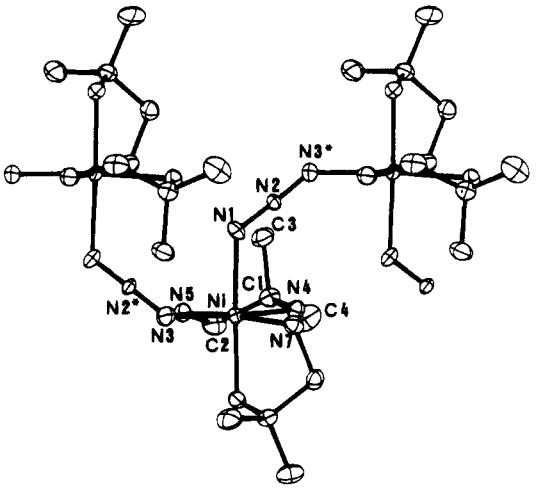

Figure 1. Atom-labeled scheme of the cationic part of $[NiL_2(\mu\text{-}N_3)]_n(ClO_4)_n$ (**1**).

Table 3. Positional Parameters and Equivalent Isotropic Thermal Parameters with Their Estimated Standard Deviations for $[NiL_2(\mu\text{-}N_3)]_n(PF_6)_n$ (**2**)

	x/a	*y/b*	*z/c*	B_{eq},[a] Å^2
Ni1	4999(5)	12226(6)	0	3.34(4)
N1	195(5)	−311(5)	80(14)	5.05(34)
N2	119(4)	−783(4)	−1208(11)	3.87(32)
N3	−95(8)	1283(5)	2541(15)	5.83(47)
N4	595(3)	2750(4)	52(18)	3.73(25)
N5	−534(4)	1557(6)	−1314(14)	3.38(31)
N6	1159(5)	1038(6)	−2280(12)	4.06(32)
N7	1604(5)	934(6)	1198(13)	4.96(38)
C1	−165(5)	3228(6)	−581(15)	4.08(37)
C2	−490(5)	2564(7)	−1970(17)	4.98(44)
C3	−701(7)	3325(7)	1002(20)	5.66(53)
C4	16(7)	4222(6)	−1427(22)	5.97(52)
C5	2221(6)	792(10)	−206(23)	6.58(62)
C6	1819(45)	517(25)	−2091(84)	15.77(406)
C6′	1922(12)	687(35)	−1840(28)	9.79(174)
C7	2966(9)	324(23)	407(33)	6.82(124)
C7′	2058(17)	−539(19)	−288(45)	7.27(131)
C8	2626(9)	1924(12)	−564(34)	9.30(102)
P	−3016(2)	1615(2)	−323(5)	5.18(13)
F1	1836(28)	3513(31)	6523(44)	16.49(243)
F1′	1613(15)	3249(16)	−3416(41)	9.16(124)
F2	−3477(26)	670(23)	−576(60)	12.80(229)
F2′	−3043(23)	466(20)	10(52)	12.44(214)
F3	−3009(26)	1821(22)	−2409(29)	10.89(151)
F3′	−3628(18)	1390(23)	−1622(46)	10.62(161)
F4	−3782(14)	2269(20)	−282(58)	13.22(181)
F4′	−2956(75)	2523(39)	−717(65)	10.66(413)
F5	−2306(14)	1040(24)	−529(39)	10.40(146)
F5′	−2239(10)	1672(20)	769(36)	10.47(124)
F6	−2697(18)	2740(17)	−183(41)	9.58(126)
F6′	−2429(22)	1458(44)	−1952(62)	16.98(291)

[a] $B_{eq} = (8\pi^2/3)\sum U_{ij}a_i^*a_j^*a_i a_j$.

Table 4. Selected Bond Lengths (Å) and Angles (deg) for $C_8H_{24}ClN_7NiO_4$ (**1**)

N1−Ni	2.160(4)	N2−N1	1.167(6)
N3−Ni	2.144(5)	N3*−N2	1.172(6)
N4−Ni	2.133(4)	N3−Ni−N1	84.9(2)
N5−Ni	2.084(5)	N2−N1−Ni	125.9(4)
N6−Ni	2.131(4)	N2*−N3−Ni	131.8(4)
N7−Ni	2.101(4)	N3*−N2−N1	177.5(4)

environment, formed by two N atoms of the two azido bridging ligands and four N atoms of the two bidentate 1,2-diamino-2-methylpropane ligands. All six Ni−N distances are similar, but two features must be underlined: the two cis Ni−N(azido) distances are the longest (2.16 and 2.14 Å), and the two shortest distances correspond to two Ni−N(amine) bonds in **trans**

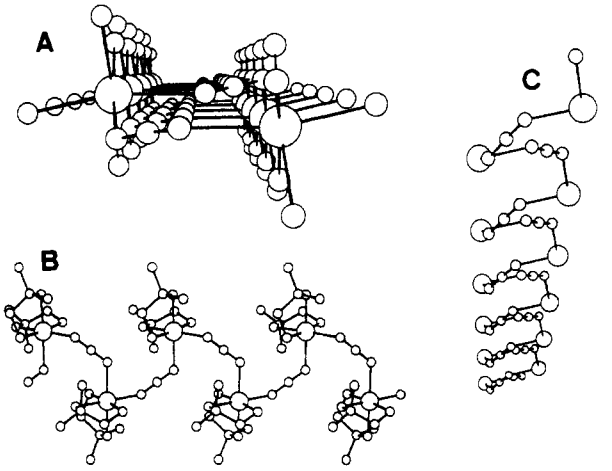

Figure 2. (A) Axial view of the cationic part of $[NiL_2(\mu\text{-}N_3)]_n(ClO_4)_n$ (**1**). (B) Perpendicular view of **1**. (C) Helicoidal nickel−azido skeleton of **1**.

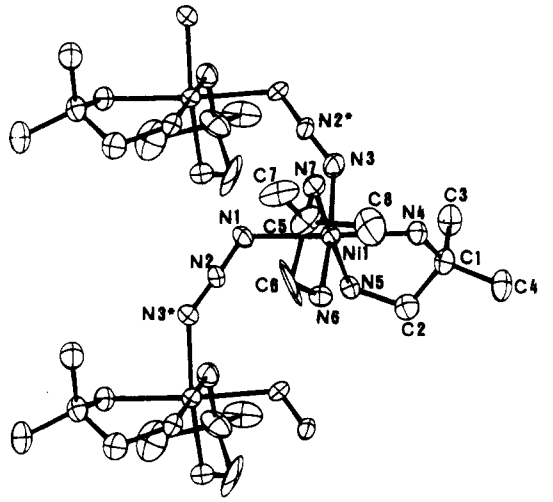

Figure 3. Atom-labeled scheme of the cationic part of $[NiL_2(\mu\text{-}N_3)]_n(PF_6)_n$ (**2**).

Table 5. Selected Bond Lengths (Å) and Angles (deg) for $C_8H_{24}F_6N_7NiP$ (**2**)

N1−Ni	2.174(6)	N2−N1	1.177(12)
N3−Ni	2.171(10)	N3*−N2	1.170(12)
N4−Ni	2.108(4)	N3−Ni−N1	84.3(2)
N5−Ni	2.072(8)	N2−N1−Ni	122.6(4)
N6−Ni	2.070(9)	N2*−N3−Ni	135.0(7)
N7−Ni	2.123(9)	N3*−N2−N1	175.1(7)

positions (Ni−N7 = 2.10 Å and Ni−N5 = 2.08 Å). The Ni−azido angles, very important from a magnetic point of view, are Ni1−N3−N2* = 131.82° and Ni1−N1−N2 = 125.90°. The torsion angle formed by Ni−NNN−Ni (calculated as the angle between the normals to the planes Ni−N1−N2−N3 and Ni*−N1−N2−N3) is 54.10°. The extension of this torsion to the 1-D system, together with the cis configurations, leads to a helicoidal nickel−azido skeleton, as shown in Figure 2. The compactness of this helix is 7.392 × 1.394 × 3.737 Å, where 7.392 Å is the distance between two Ni(II) nonconsecutives (Ni1−Ni3); 1.394 Å is the distance from Ni to the N1,N2,-N3*,Ni* mean plane, and 3.737 Å is the distance from Ni* to the Ni,N4,N5,N7,N3 mean plane.

$[NiL_2(\mu\text{-}N_3)]_n(PF_6)_n$ (2). A labeled scheme is shown in Figure 3. The main bond lengths and angles are listed in Table 5. Other distances and angles may be found in the Supporting Information. The nickel atom occupies a distorted octahedral environment, formed by two N atoms of the two azido bridging

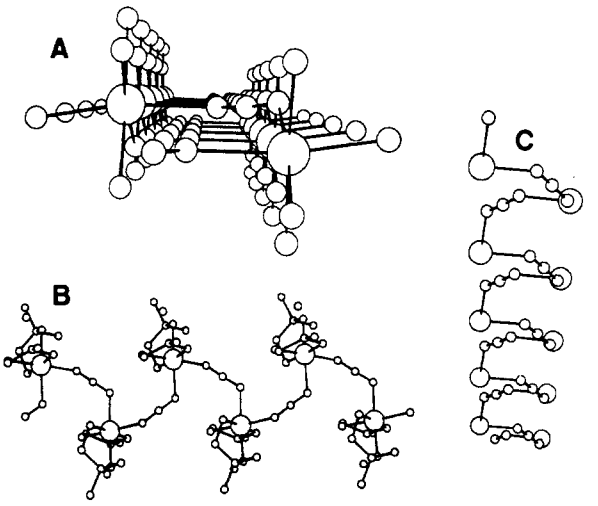

Figure 4. (A) Axial view of the cationic part of $[NiL_2(\mu\text{-}N_3)]_n(PF_6)_n$ (**2**). (B) perpendicular view of **2**. (C) Helicoidal nickel–azido skeleton of **2**.

ligands and the four N atoms of the two bidentate 1,2-diamino-2-methylpropane ligands. All six Ni–N distances are similar, but two features should be underlined: the two cis Ni–N(azido) distances are the longest (2.16 and 2.14 Å), and the two shortest distances correspond to two Ni–N(amine) bonds in **cis** positions (Ni–N5 = 2.072 Å and Ni–N6 = 2.07 Å). The Ni–azido angles, very important from magnetic point of view are Ni1–N3–N2* = 135.04° and Ni1–N1–N2 = 122.62°. The torsion angle formed by Ni–NNN–Ni, defined as above, is 53.21°. The extension of this torsion to the 1-D system, together with the cis configurations, leads to a helicoidal nickel–azido skeleton (Figure 4). The compactness of this helix, defined as above, is 7.550 × 1.471 × 3.772 Å.

Magnetic Properties. The molar magnetic susceptibilities vs T for **1** and **2** are plotted in Figure 5. For **1**, the molar susceptibility value (3.82×10^{-3} cm^3 mol^{-1} at room temperature) increases when the temperature decreases, reaching a maximum of 1.31×10^{-2} cm^3 mol^{-1} at 30 K, and below this temperature the curve decreases continuously to 8.32×10^{-3} cm^3 mol^{-1} at 4 K. For **2**, the behavior is different: the χ_M vs T plot increases continuously to 4 K. At room temperature the value of χ_M is 4.45×10^{-3} cm^3 mol^{-1}, and at 4 K it is 1.38×10^{-1} cm^3 mol^{-1}. The $\chi_M T$ value decreases from 1.11 cm^3 K mol^{-1} (300 K) to 0.04 cm^3 K mol^{-1} (5 K) for the perchlorate and from 1.294 cm^3 K mol^{-1} (300 K) to 0.055 cm^3 K mol^{-1} (4.2 K) for the hexafluophosphate chains, tending to zero. The continuous decrease in the $\chi_M T$ value and the maximum observed in the thermal variation of the molar susceptibility for **1** clearly indicate the existence of strong antiferromagnetic intrachain interactions in the perchlorate **1** and very weak ones in the hexafluorophosphate **2**, respectively.

The more general spin Hamiltonian to describe the magnetic properties of isotropic Ni(II) chains, taking into account the single-ion terms and the interactions between the nearest-neighbor center, is

$$H = \sum_i (\beta \hat{S}_i \cdot g_i \vec{H} - J \hat{S}_i \cdot \hat{S}_{i+1})$$

The terms corresponding to the anisotropic exchange and antisymmetric exchange have not been considered because these effects are only relevant at very low temperatures (near 2 K).

There is no exact mathematical expression for χ_M vs T of infinite isotropic Heisenberg chains. Nevertheless, there exist numerical calculations that approximately characterize the

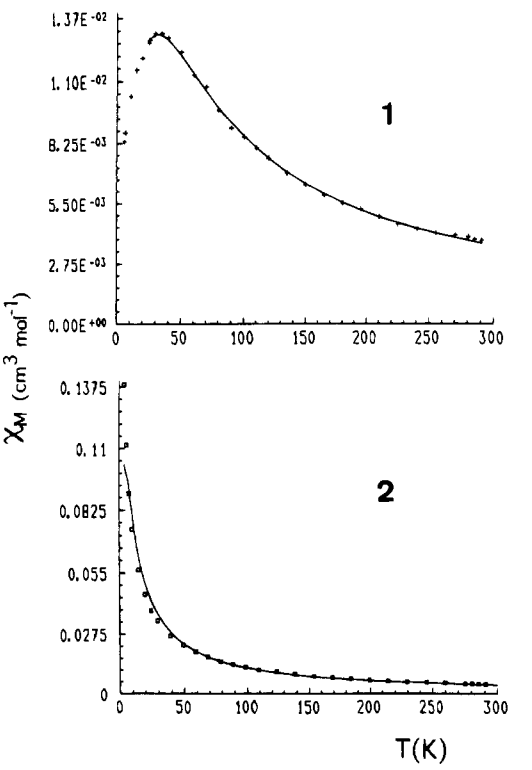

Figure 5. Magnetic susceptibility plots of a polycrystalline sample for $[NiL_2(\mu\text{-}N_3)]_n(ClO_4)_n$ (**1**) and for $[NiL_2(\mu\text{-}N_3)]_n(PF_6)_n$ (**2**). Solid lines show the best fit (see text).

Heisenberg behavior in 1-D systems.[21,22] For $S = 1$ the characteristic expressions are[23]

$$\frac{kT(\chi_{max})}{|J|} \approx 1.35 \quad (1)$$

$$\frac{\chi_{max}|J|}{Ng^2\beta^2} \approx 0.176 \quad (2)$$

For **1**, by substitution of the experimental data $T(\chi_{max})$ [temperature corresponding to the maximum in susceptibility] = 30 K, χ_{max} = 0.01306 cm^3 K mol^{-1}, and considering g = 2.20 (usual for octahedral Ni(II) complexes), we obtain J = −15.4 cm^{-1} in (1) and J = −16.3 cm^{-1} in (2).

In the case of isotropic 1-D $S = 1$ systems, the temperature dependence of the susceptibility extrapolated from calculations performed on ring systems of increasing length has been given by Weng.[24] Our experimental data were then fitted to the Weng equation

$$\chi_M = \frac{N\beta^2 g^2}{kT} \frac{2 + 0.019\alpha + 0.777\alpha^2}{3 + 4.346\alpha + 3.232\alpha^2 + 5.834\alpha^3} \quad (3)$$

$$\alpha = |J|/kT$$

This formula is only valid for an antiferromagnetic coupling and only if the nickel ion is magnetically isotropic. A good fit is only possible down to temperatures near the maximum of X (in our case near 30 K for **1** and, taking into consideration that there is no maximum, near 10 K for **2**) because neither zero-field splitting nor the Haldane gap effect[25] is taken into account in the equation. The J values were obtained by minimizing

(21) Blöte, H. W. *J. Am. Chem. Soc.* **1964**, *32*, 343.
(22) De Neef, T.; Kuipers, A. J. M.; Kopinga, K. *J. Phys.* **1974**, *A7*, L171.
(23) Carlin, R. L. *Magnetochemistry*; Springer-Verlag: Berlin, 1968; p 178.
(24) Weng, C. Y. Ph.D. Thesis, Carnegie Institute of Technology **1968**.

the function $R = \Sigma(\chi_M^{calc} - \chi_M^{obs})^2/\Sigma(\chi_M^{obs})^2$. The best fitted parameters obtained are $J = -16.8$ cm^{-1}, $g = 2.19$, and $R = 1.2 \times 10^{-4}$ for **1** and $J = -3.25$ cm^{-1}, $g = 2.24$, and $R = 7 \times 10^{-4}$ for **2**.

Interpretation of the Magnetic Results. In previous studies magneto–structural correlations in end-to-end trans- and cis-azido Ni(II) chains have been reported.[13,17] The three main factors are the Ni–N–N angles, the Ni–NNN–Ni torsion angle, and the Ni–N(azido) distances. For the Ni–N–N angle, the maximum coupling is expected for $\alpha \approx 108°$. For greater α values (as found experimentally), the antiferromagnetic interaction must decrease. An accidental orthogonality valley, centered on $\alpha = 165°$, was observed. The effect of the Ni–N_3–Ni torsion angle was also parametrized. For all α values, the maximum coupling can be expected for a torsion value of zero, decreasing gradually when the torsion angle increases. The magnitude of this effect is lower than the effect of the bond angle. Finally, calculations varying *d* (Ni–N distance) in the range 2.02–2.20 Å indicate that, for greater distances, lower antiferromagnetic values occur. For example, a variation of *d* between 2.09 and 2.21 Å reduced the antiferromagnetic coupling by ca. 35%.

Consequently, the factors that can be related to the magnetic behavior are in this case (a) the coincident **average** value of Ni–N–N values for both structures, 128.86° for **1** and 128.83° for **2**, respectively, representing an intermediate *J* value, equal for the two compounds; (b) the high values of the Ni–N_3–Ni torsion angles (54.10 and 53.21°, respectively) which must give almost equal and low antiferromagnetic coupling; and (c) the Ni–N(azido) distances, which are 2.144 and 2.160 Å for **1** and 2.174 and 2.171 Å for **2**, respectively.

If we consider only these three factors to explain the different magnetic behaviors of the two complexes (*J* values from ca. -17 cm^{-1} for **1** and ca. -3 cm^{-1} for **2**), we realize that all these three factors are very similar. On the other hand, factors b and c act in the opposite directions: the ClO_4^- chain has a greater torsion angle and shorter *d* distances, and the PF_6^- chain has a smaller torsion angle but longer *d* distances. The two factors may compensate for each other and would thus not explain the difference in magnetic behavior.

If we consider the short-range order in the chains, the only remarkable difference between the two chains is the difference in compactess, as defined above: 7.392 × 1.394 × 3.737 Å for **1** and 7.550 × 1.471 × 3.772 Å for **2**. This difference is due to the sum of all the small differences in angles and distances, which is difficult to visualize independently, for **1** and **2**. The more compact the helicoidal structure, the greater the antiferromagnetic coupling.

Finally, there is another important electronic factor not explained in previous studies on similar systems:[13,17] the different positions of the magnetic orbitals in consecutive Ni(II) ions in the two 1-D complexes. In **1**, as pointed out above, the octahedron can be described as compressed in trans-N(amine) positions, assuming that this direction corresponds to the *z* axis. The magnetic pathway is, thus, the operative d_{xy}–d_{xy}. In contrast, in **2** the octahedral distortion is not an axial elongation or compression. The mixing of d_{z^2} and d_{xy} is more pronounced, giving two possible magnetic pathways: d_{xy}–d_{xy} (as in **1**) and d_{z^2}–d_{xy}, which reduces the overlap and, thus, the antiferromagnetic coupling.

In summary, the two last factors could be assumed to be responsible for the differences in magnetic properties: the tetrahedral perchlorate anion allows greater compactess, creating more antiferromagnetic coupling, enhanced by the operative d_{xy}–d_{xy} magnetic pathway. In contrast, the larger hexafluorophosphate anion allows lower compactness, which creates lower antiferromagnetic coupling, diminished by the less-operative d_{xy}–d_{z^2} magnetic pathway. The sum of all factors may explain the different magnetic behaviors for **1** and **2**. More cis-azido complexes are necessary to show that this electronic factor (mixing of d orbitals) is the main one in some cases. Relevant research is currenly under way in our laboratory.

Acknowledgment. We are very grateful for the financial assistance from the CICYT (Grant PB93-0772).

Supporting Information Available: Tables giving crystal data and details of the structure determination, anisotropic thermal parameters, bond angles and distances, and hydrogen atom coordinates (14 pages). Ordering information is given on any current masthead page.

IC9407353

(25) (a) Haldane, F. D. M. *Phys. Rev. Lett.* **1983**, *50*, 1153. (b) Haldane, F. D. M. *Phys. Lett.* **1983**, *93A*, 464. (c) Renard, J. P.; Verdaguer, M.; Regnault, L. P.; Erkelens, W. A. C.; Rossat-Mignon, J.; Stirling, W. G. *Europhys. Lett.* **1987**, *3*, 945. (d) Renard, J. P.; Verdaguer, M.; Regnault, L. P.; Erkelens, W. A. C.; Rossat-Mignon, J.; Ribas, J.; Stirling, W. G.; Vettier, C. *J. Appl. Phys.* **1988**, *63*, 3538.